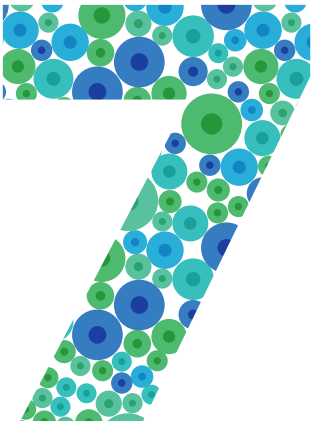

Carboplatin-paclitaxel chemotherapy selectively depletes circulating myeloid cells in high-grade serous ovarian cancer patients

FL Komdeur*, FA Eggink*, KL Brunekreeft, A Plat, EJ Propper, HH Workel, N Leffers, M de Bruyn, HW Nijman

*Authors contributed equally

Submitted

ABSTRACT

High-grade serous ovarian cancer (HGSOC) is the most lethal gynecological malignancy with limited therapeutic options. While trials exploring immunotherapy in HGSOC are promising, clinical efficacy remains restricted to a small percentage of patients. Several lines of evidence suggest that this low response rate might be improved by incorporating immunotherapy into standard-of-care chemotherapy for HGSOC, consisting of carboplatin and paclitaxel. To address whether this approach might be feasible, we analysed the systemic effects of first line carboplatin/paclitaxel chemotherapy on 35 immune markers in HGSOC patients pre-, mid- and post-chemotherapy. HGSOC patients had baseline immune profiles consistent with their advanced age, including a high relative ratio of myeloid to lymphocyte cells, but did not differ significantly from age-matched controls. A significant decrease in the relative abundance of the myeloid compartment of HGSOC patients was observed during carboplatin/paclitaxel treatment, which rebounded slightly after completion of chemotherapy. Depletion was uniform across all major myeloid subsets. No changes were observed in the relative abundance of other immune cell subsets, and T cell proliferation was not negatively affected by carboplatin/paclitaxel. Our data suggest carboplatin/paclitaxel chemotherapy might potentiate immunotherapy in the neo-adjuvant treatment of HGSOC through depletion of myeloid cells.

INTRODUCTION

High-grade serous ovarian cancer (HGSOC) is the most lethal gynecological malignancy and the fifth leading cause of cancer death in women. Almost all HGSOC patients present with advanced stage of disease and relapse rates are high with a 5-year survival of only 35%.[1] This poor prognosis for women with HGSOC has not improved in decades and new therapies are urgently needed. A promising new approach for the treatment of HGSOC may be immunotherapy.

Indeed, the immune system plays an important role in the development and control of HGSOC, and the number of intraepithelial CD8+ T cells in particular is associated with prolonged survival.[2–4] In addition, differentiation, exhaustion and other functional parameters of these intraepithelial CD8+ T cells have all been associated with prognosis, as has the presence of regulatory T cells, macrophages, B cells, myeloid-derived suppressor cells and others.[5–9] As in many tumor types, the immune checkpoint programmed death 1 (PD-1) and its ligand PD-L1 are also associated with prognosis, although controversy on the direction of this effect remains.[10–14] Nevertheless, initial trials using blocking antibodies (immune checkpoint blockade; ICB) targeting PD-1 or PD-L1 have demonstrated clinical effect in HGSOC patients, albeit in a small percentage of patients.[15] One potential strategy to increase the efficacy of immunotherapy, including ICB, is to combine treatment with other modalities, such as chemotherapy.

In HGSOC, a combination of carboplatin and paclitaxel chemotherapy is the standard of care for treatment of patients with advanced disease worldwide. Carboplatin and paclitaxel are DNA intercalating and cell cycle inhibitors, respectively, used frequently in combination for the treatment of ovarian, endometrial, lung and breast cancers. For HGSOC patients, carboplatin/paclitaxel is administered in 6 cycles of 3 weeks and combined with cytoreductive surgery performed either prior to chemotherapy, or at the interval (i.e. after 3 cycles of chemotherapy; see also supplementary Figure 1A and 1B). Previously, we demonstrated that the number and differentiation of tumor-infiltrating lymphocytes (TIL) did not differ between tumours that were carboplatin/paclitaxel-naïve when compared with tumours isolated after 3 cycles of chemotherapy.[16,17] Further, Lo et al. recently demonstrated that TIL+ tumours even showed an increase in the number of TIL after carboplatin/paclitaxel chemotherapy, whereas TIL- tumours did not, suggesting carboplatin/paclitaxel augments existing anti-tumour immunity.[18] However, little longitudinal data exists on the systemic immune cell status of HGSOC patients undergoing carboplatin/paclitaxel chemotherapy.

In this study, we analysed the effects of carboplatin/paclitaxel chemotherapy on the immune cell composition of HGSOC patients by evaluating 35 immune cell markers pre-, mid- and post-chemotherapy.

RESULTS

Carboplatin/paclitaxel chemotherapy selectively depletes myeloid cells from the circulation

A total of 75 patients with suspected ovarian cancer participated in the study. HGSOC was diagnosed in 18 of these patients. Consecutive pre- and post-chemotherapy samples were available in 7 patients (Table 1). First, we performed unbiased analyses of changes in the immune cell composition of the peripheral blood of HGSOC patients during carboplatin/paclitaxel chemotherapy. Hereto, PBMCs from HGSOC patients were isolated before chemotherapy, after 3 cycles of chemotherapy, and/or after completion of all 6 cycles of chemotherapy. PBMCs were screened by flow cytometry using validated antibodies against 35 major immune cell markers (supplementary table 1) in combinations of 8 distinct flow cytometry panels (supplementary table 2). After manual gating on live single cells of myeloid/lymphocyte size and density (supplementary Figure 1C), a previously described unsupervised clustering algorithm for identifying differences between different treatment groups in high-dimensional flow cytometry data (CITRUS) was used for analysis of each flow cytometry panel separately, totalling 8 analyses of up to 7 markers per analysis.[19]

Initial assessment of T cell differentiation (Figure 1A; panel 1, supplementary table 2) revealed no significant changes in T cell prevalence or differentiation during chemotherapy. However, a significant change was observed in the non-lymphocytic subset of $CD95^{high}$ / $CD4^{int}$ / FSC^{high} / SSC^{high} cell clusters, consistent with a myeloid cell population (Figure 1B and 1C). A significant relative decrease of clusters I and II was observed after 3 cycles of chemotherapy which rebounded slightly after 6 cycles of chemotherapy (Figure 1D). Back-gating and overlay of the identified cell clusters onto the total dataset similarly revealed these cells to be of myeloid cell size and density, with a specific loss from the total leukocyte population during chemotherapy treatment (exemplified for one patient in Figure 1D). Further, manual assessment of the data using standard gating strategies revealed a similar and significant relative depletion of myeloid cells compared to lymphocytes during chemotherapy (Figure 1E and supplementary Figure 1D). Of note, comparing age-matched patients with a benign ovarian tumour to HGSOC patients revealed no significant differences in the relative myeloid cell fraction (supplementary Figure 1E), nor did any other CITRUS analysis comparing baseline HGSOC samples to age-matched controls. Together, these data suggest that the relative expansion of the myeloid cells in the HGSOC population is due to cancer-unrelated patient-specific changes. Indeed, baseline percentages of myeloid cells varied extensively between individuals with HGSOC and benign tumours (Figure 1F and Supplementary Figure 1E).

TABLE 1. Patient characteristics

Age (years)	Stage (FIGO)	Grade	Histology	CA125 level	Primary treatment	Residual disease (cm)	Follow up status	DSS (months)	PFS (Months)
62	IIIc	grade III	serous	215	PS	0	ED	48	41
72	IIIc	grade III	serous	1771	PS	0	NED	39	39
60	IIc	grade II	serous with clearcell component	238	PS	0	NED	34	34
59	IIIc	grade III	serous	17776	NACT	0	NED	31	31
64	IIIc	grade III	serous	1287	PS	0	ED	26	18
52	IIIc	grade III	serous	470	PS	0	NED	11	11
75	IIIc	grade III	serous	432	NACT	0	ED	12	12

PS: primary cytoreductive surgery; followed by 6 cycles carboplatin/paclitaxel chemotherapy. chemotherapy.
NACT: neoadjuvant chemotherapy; 3 cycles carboplatin/paclitaxel chemotherapy followed by cytoreductive surgery and 3 additional cycles of carboplatin/paclitaxel
NED: no evidence of disease. ED: evidence of disease DSS: disease specific survival. PFS: progression free survival

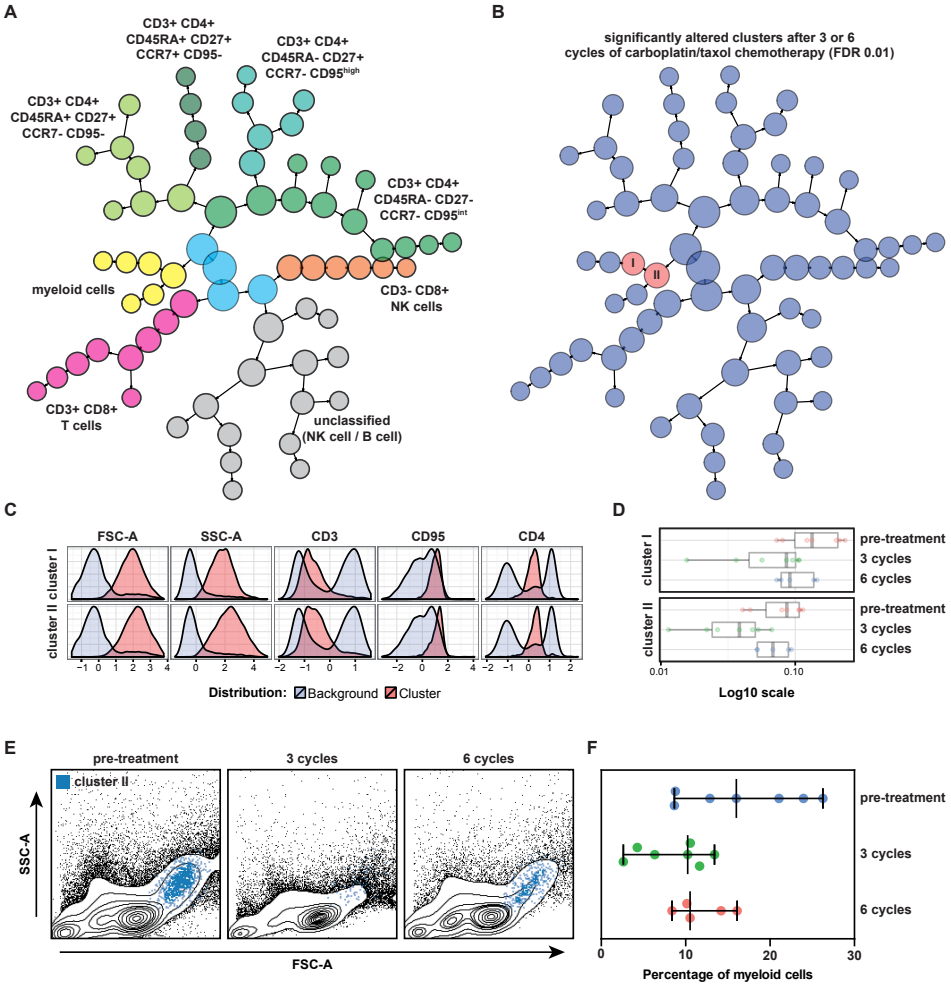

FIGURE 1. Carboplatin/paclitaxel selectively depletes myeloid cells from the circulation. Unsupervised hierarchical clustering of PBMCs was performed using CITRUS based on FSC and SSC light scatter characteristics, and expression of CD3, CD4, CD8, CD45RA, CCR7, CD27 and CD95 (panel 1, supplementary table 2). **A)** Identified clusters were assigned to specific immune cell subsets and pseudocolored based on expression of CD3, CD4, CD8, CD45RA, CCR7, CD27 and CD95. **B)** Clusters significantly altered between pre-, mid- and post-chemotherapy samples are highlighted in red (I and II) **C)** Phenotype of significantly altered cluster I and II and **D)** prevalence of cluster I and II at the indicated time-points. **E)** Events from cluster I and II were exported and overlaid on the total dataset of the individual patients and time-points to confirm the phenotype (illustrated for 1 patient). **F)** Manual gating and quantification of myeloid cells based on FSC and SSC light scatter characteristics.

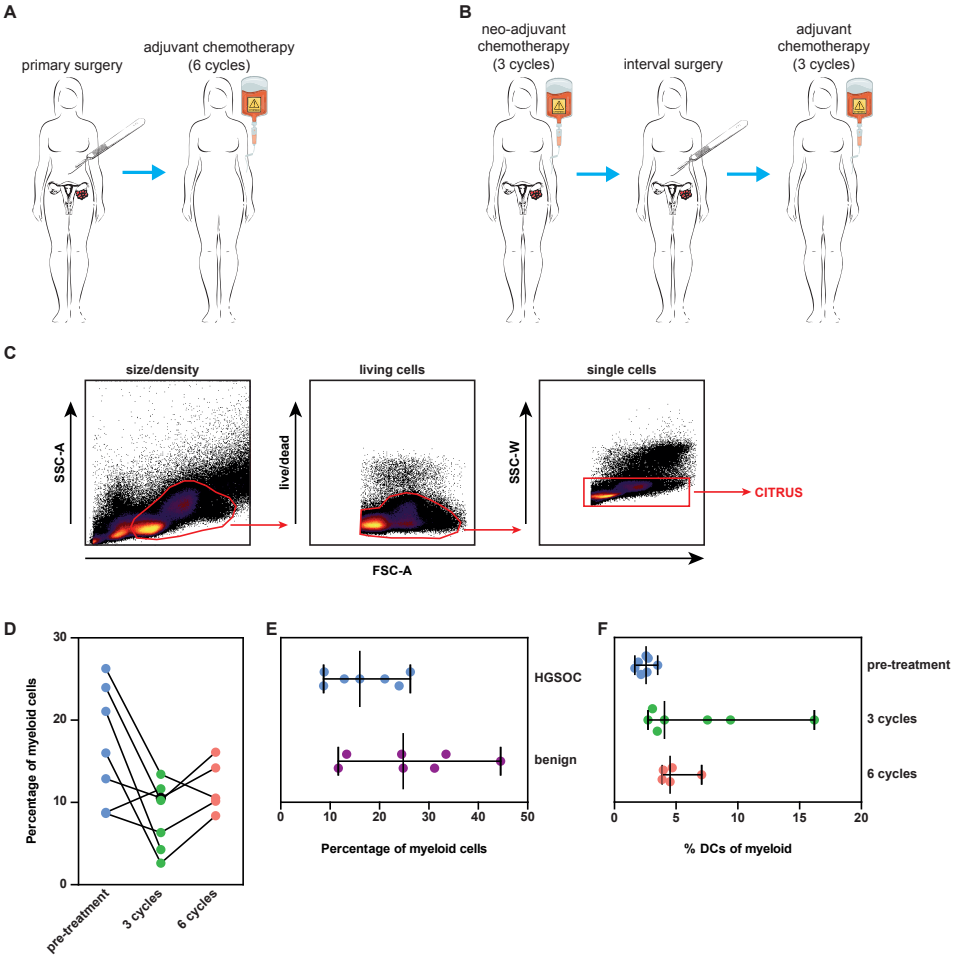

SUPPLEMENTARY FIGURE 1. Carboplatin/paclitaxel selectively depletes myeloid cells from the circulation. A-B) Treatment scheme for high-grade serous ovarian cancer patients included in this study. **C)** Gating strategy used for preselecting events for analysis by CITRUS. **D)** Manual gating and quantification of myeloid cells based on FSC and SSC light scatter characteristics for each individual patients per time point. **E)** Manual gating and quantification of myeloid cells based on FSC and SSC light scatter characteristics comparing HGSOC and age-matched control with benign ovarian tumours. **F)** Percentage of Lineage-negative HLA-DR+ cells as a fraction of the total myeloid population at the indicated time-points.

Carboplatin/paclitaxel chemotherapy depletes cells evenly across all major myeloid subpopulations

In line with the above, analysis of major myeloid cell populations using a myeloid-directed antibody panel (panel 2; supplementary table 2) also revealed a significant decrease in the percentage of circulating myeloid cells after carboplatin/paclitaxel chemotherapy (Figure 2A). This change was present only in a root cluster, but not linked to specific myeloid subsets (Figure 2A). In line with this, the identified clusters showed a remarkably homogenous phenotype of $CD14^{+}$ / $CD11b^{+}$ / $CD11c^{+}$ /$CD33^{+}$ / HLA-DR^{+} / FSC^{high} /SSC^{high}, consistent with circulating monocytes (Figure 2B). The relative depletion of myeloid cells observed using these myeloid markers was similar as that observed when analysing T cell differentiation markers as described above, indicating the use of "basic" FSC and SSC characteristics may already be sufficient to assess the carboplatin/paclitaxel-induced myeloid cell depletion (Figure 2C).

To confirm that carboplatin/paclitaxel did not have a specific and negative effect on circulating antigen-presenting dendritic cell subsets (DCs), we also analysed major DC markers (supplementary table 1 and 2) using CITRUS and visualized the distribution of the subsets using t-Distributed Stochastic Neighbour Embedding (t-SNE) followed by manual gating for all patients and time-points (exemplified in Figure 2D). No differences were observed in DC abundance by CITRUS. In a single patient, we observed a marked expansion of CD11c+ CD1c- mDCs after 6 cycles of chemotherapy (Figure 2D and 2E), but most other effects observed were minimal and similarly heterogeneous (Figure 2E), in line with the initial CITRUS analysis. Thus, DC subsets were not specifically depleted by chemotherapy in these patients, slightly shifting the relative ratio of DC over monocyte in favour of DCs (supplementary Figure 1F).

Carboplatin/paclitaxel chemotherapy in HGSOC has minimal effects on T cell phenotype and function

Finally, we assessed how carboplatin/paclitaxel chemotherapy affects T cell phenotype and function using a combination of T cell activation, differentiation and exhaustion markers specific for both CD4 and CD8 T cells (panel 6, supplementary table 2). In addition, we assessed markers previously associated with improved prognosis and/or response to immunotherapy in other malignancies (panels 4-7, supplementary table 2). In line with the initial unsupervised analysis, no consistent changes in T cell markers were observed across all patients and time-points analysed for either CD4 (Figure 3A) or CD8 cells (Figure 3B).

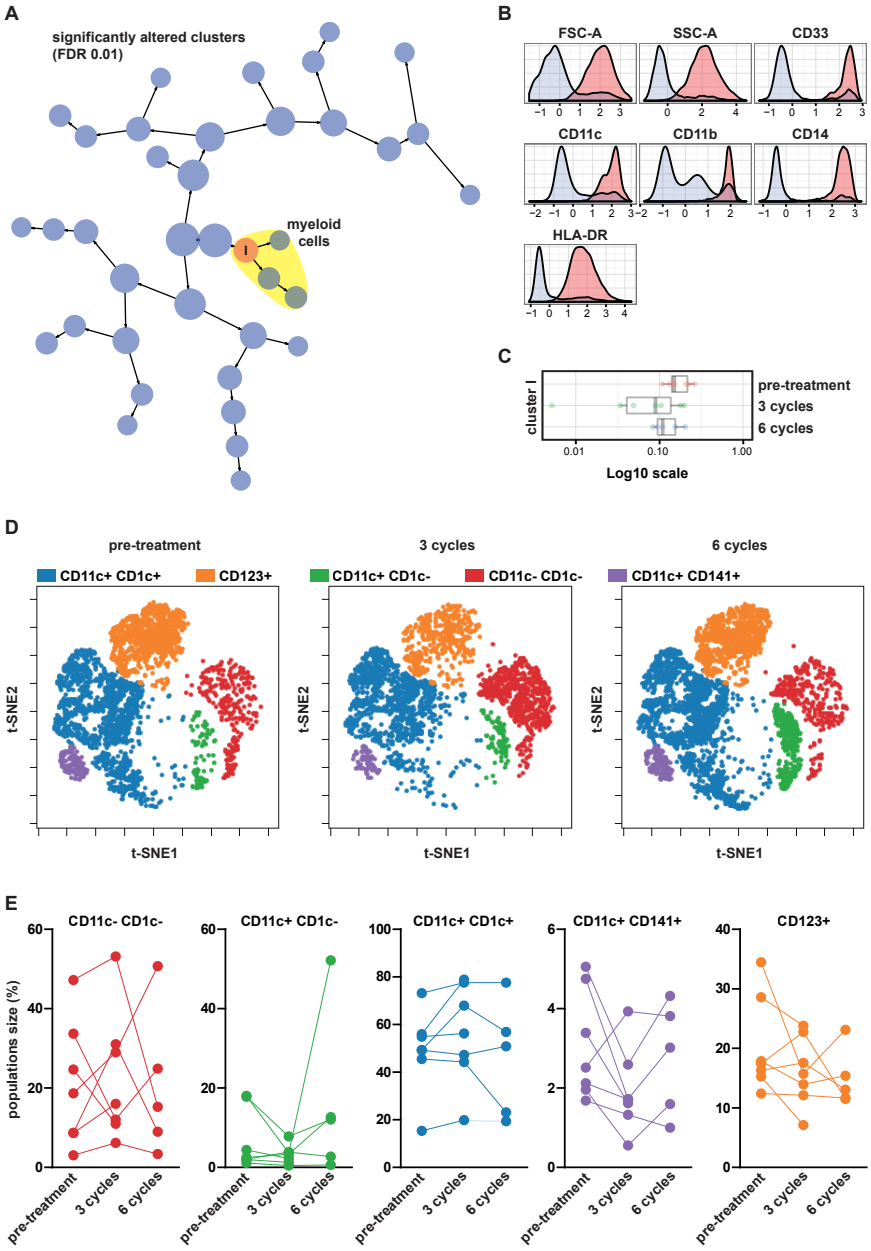

FIGURE 2. Carboplatin/paclitaxel depletes myeloid cells evenly across all major subpopulations. Unsupervised hierarchical clustering of PBMCs was performed using CITRUS based on FSC and SSC light scatter characteristics, and expression of CD33, CD14, CD11c, CD11b and HLA-DR (panel 2, supplementary table 2). **A)** Clusters significantly altered between pre-, mid- and post-chemotherapy samples are highlighted in red (I) **B)** Phenotype of significantly altered cluster I and **C)** prevalence of cluster I at the indicated time-points. **D)** PBMCs were gated based on a Lineage-negative HLA-DR+ phenotype and DC subpopulations identified using t-Distributed Stochastic Neighbour Embedding (t-SNE) on the basis of CD11c, CD123, CD141 and CD1c expression. **E)** Quantification of the identified DC populations for individual patients and time-points.

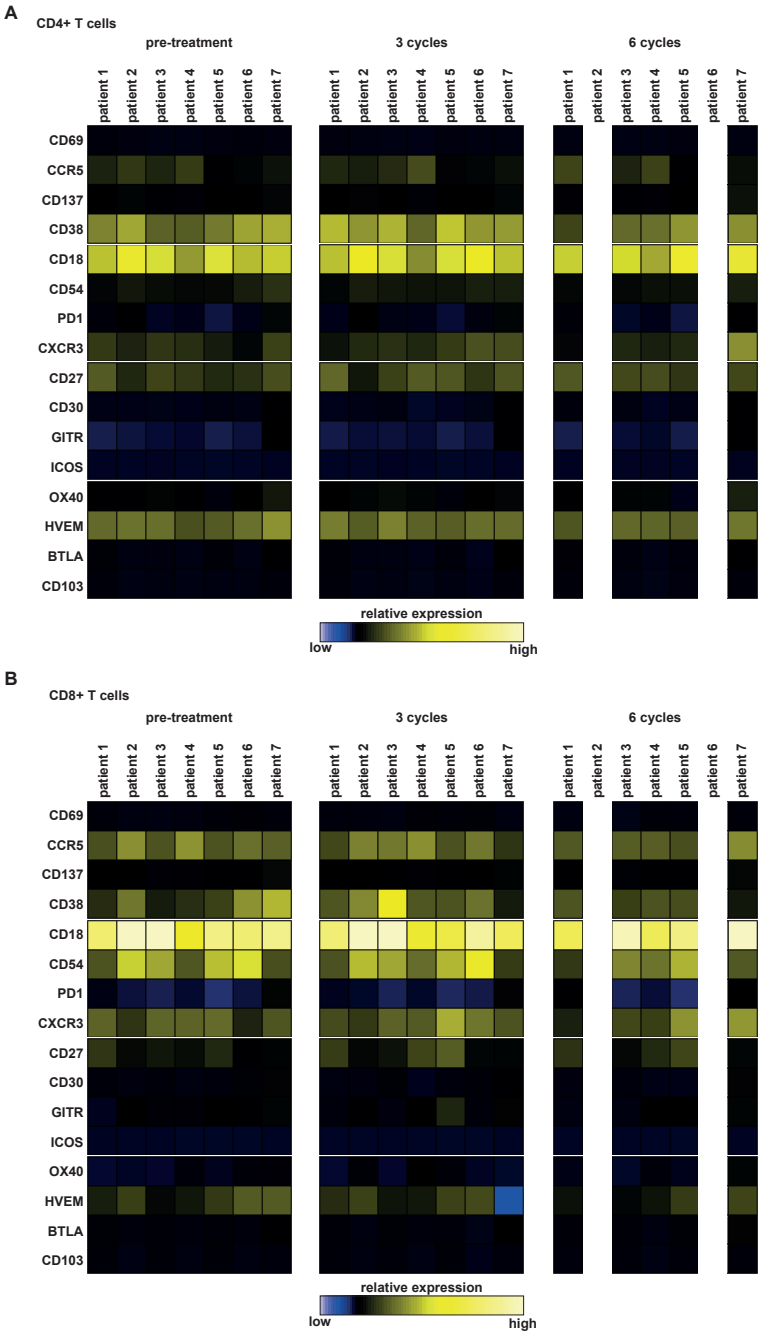

FIGURE 3. Carboplatin/paclitaxel has minimal effects on T cell phenotype. A) CD4 and **B)** CD8+ T cells were identified based on expression of CD3 and CD4 or CD8 and expression of the indicated markers assessed in each of the two cell populations using mean fluorescent intensity (panels 4-7, supplementary table 2).

Moreover, carboplatin/paclitaxel chemotherapy did not affect the proliferation of T cells as determined by Ki67 staining (Figure 4A; panel 8, supplementary table 2), the relative expression of key transcription factors EOMES and Tbet (Figure 4B), nor the activation and expansion of T cells in response to stimulation with anti-CD3/anti-CD28 beads in combination with low dose IL-2 (Figure 4C). Lastly, the proportion of regulatory FoxP3+ T cells and their proliferative capacity was also not affected in this patient cohort (Figure 4A). Taken together, our data suggests T cell phenotype and function remain unaffected by the administration of carboplatin/paclitaxel chemotherapy in HGSOC patients.

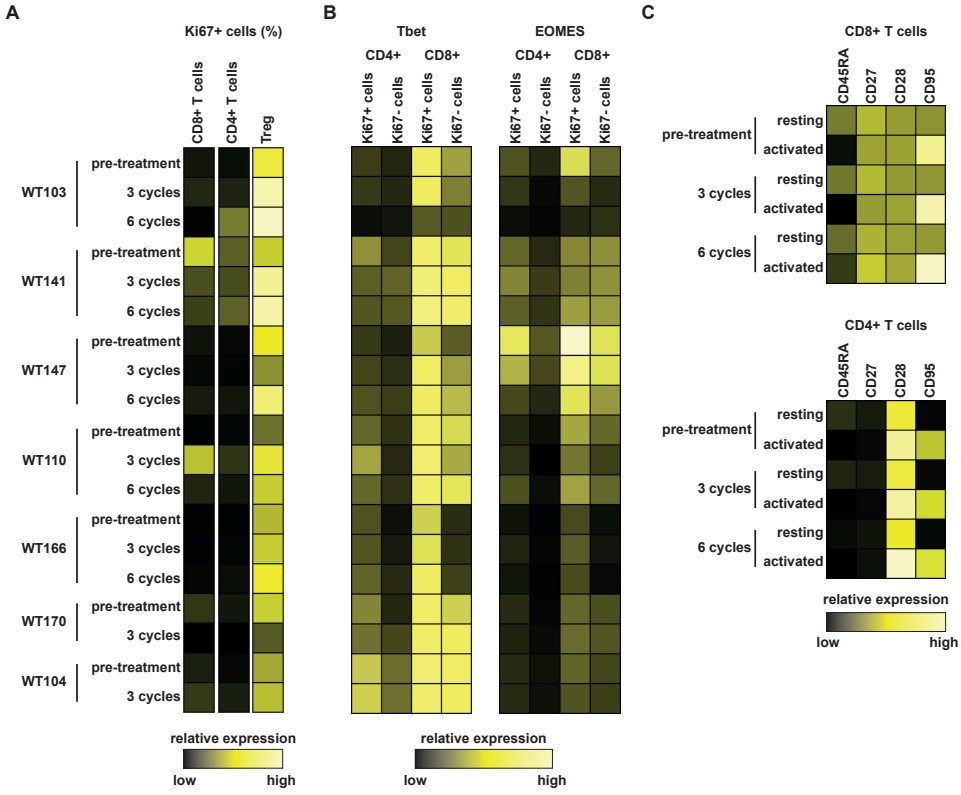

FIGURE 4. Carboplatin/paclitaxel has minimal effects on T cell activity. A-B) CD4 and CD8+ T cells were identified based on expression of CD3 and CD4 or CD8 and expression of Ki67, Tbet and/or EOMES assessed using mean fluorescent intensity as indicated (panel 8, supplementary table 2). **C)** PBMCs from one of the patients at 3 individual time-points were stimulated *ex vivo* using anti-CD3/anti-CD28 beads in the presence of 100 U/mL IL-2 and T cell activation and differentiation markers assessed as indicated. **D)** Percentage of FoxP3+ CD4+ cells for all patients at all time-points.

DISCUSSION

In the current study we demonstrate that carboplatin/paclitaxel chemotherapy specifically depletes myeloid cells from the circulation of HGSOC patients. Depletion does not appear to affect any major myeloid subset in particular and shifted the relative ratio of DCs to total myeloid cells in favour of DCs. In addition, we establish that carboplatin/paclitaxel chemotherapy does not affect T cell phenotype, activation or differentiation in HGSOC patients at the indicated time-points.

Our data is in line with a report on the effect of carboplatin/paclitaxel treatment in cervical cancer patients.[20] In that study, Welters et al. described an expansion of myeloid cells in advanced cervical cancer patients compared to healthy controls, which normalized after carboplatin/paclitaxel chemotherapy. This effect was also associated with increased T cell reactivity to recall antigens. Interestingly, the baseline magnitude of myeloid cell expansion appears to be more pronounced in cervical cancer, with some patients having almost 70% of myeloid cells at baseline, and a median of ~50% compared to a median of ~16% observed in our patients. This difference in magnitude may also explain why Welters et al. observed an increase in circulating myeloid cells compared to healthy donors while this difference did not reach statistical significance in our set. Despite these differences, the magnitude and timing of the observed decrease in myeloid cells are remarkably consistent between cervical and HGSOC patients with a more pronounced depletion during chemotherapy that rebounds somewhat after conclusion of all 6 cycles. Since the depletion of myeloid cells in cervical cancer patients also enhanced the proliferative HPV16-specific T cell responses after a therapeutic vaccination, this suggests a rationale for combining carboplatin/paclitaxel with e.g. immune checkpoint inhibitors or tumour antigen-specific vaccination in the neo-adjuvant treatment setting of HGSOC.[21]

There are a number of potential explanations for the decreased number of myeloid cells during chemotherapy Firstly, carboplatin/paclitaxel has a well-established toxicity profile that includes a decreased leukocyte output from the bone marrow resulting in leukopenia in some patients.[22] Indeed, some, but not all, of the patients included in our analysis displayed leukopenia during treatment (data not shown), although we did not observe a direct correlation with the magnitude or timing of myeloid cell depletion and leukopenia. Nevertheless, the half-life of myeloid cells in circulation (1-3 days) would render them more sensitive to depletion by reduced bone-marrow output when compared to e.g. lymphocytes with an estimated half-life of between 1 month and 8 years depending on the subset.[23–25] Alternatively, the decreased tumour burden after chemotherapy and/or cytoreductive surgery may reduce the release of cancer-produced factors from the tumour that induced the initial myeloid expansion. Indeed, release of IL-6 and/or IL-10 from ovarian cancer cells has been linked to reduced HLA-DR levels on circulating $CD14^+$ monocytes and acquisition of myeloid-derived suppressor cell (MDSC) function.[26] Nevertheless,

while we have previously detected such a $CD14^+$ HLA-DR^{low} population in HGSOC tumours (unpublished data), we did not observe this MDSC population in the circulation here. Further, our data on age-matched controls suggests the expansion of myeloid cells in these patients may be independent of tumour-derived factors. Finally, the combination of carboplatin/paclitaxel may have direct effects on the myeloid cell populations. While the cytotoxic effects of carboplatin/paclitaxel on myeloid cells has not been described as particularly higher than those observed in lymphocytes, auto- and/or paracrine effects have been described to skew monocyte differentiation and/or migration, potentially through IL-6- and PGE2-dependent mechanisms.[27]

Importantly, we observed no deleterious effects of carboplatin/paclitaxel on differentiation, activation and/or proliferation of T cells, confirming previous reports that certain chemotherapeutic regimes can be effectively combined with T cell-targeting immunotherapy.[20,21,28] Indeed, combined carboplatin/paclitaxel with immune checkpoint inhibitors in the neo-adjuvant treatment of breast cancer appears well tolerated and efficacious.[28]

In conclusion, our data suggests carboplatin/paclitaxel chemotherapy fosters a permissive environment for immunotherapeutic intervention in the neo-adjuvant treatment setting of HGSOC by depleting myeloid cells without affecting T cells. These findings have direct implications for the design of immunotherapy trials in HGSOC patients.

MATERIALS AND METHODS

Patients and ethics

PBMCs from HGSOC patients were isolated before carboplatin/paclitaxel chemotherapy, 1-3 weeks after 3 cycles of chemotherapy, and 4-6 weeks after completion of all 6 cycles of chemotherapy. PBMCs were isolated by ficoll density centrifugation using lymphoprep according to the manufacturer's instructions. As a control, PBMCs were isolated from age-matched patients with a benign ovarian tumour. According to Dutch law, approval from our institutional review board was obtained. Subsequently, all patients gave written informed consent and data was collected in an anonymous database in which patient identity was protected by unique patient codes.

Flow cytometric analysis

PBMCs were characterized by multiparameter flow cytometry. The Zombie Aqua Fixable Viability Kit (BioLegend, Uithoorn, The Netherlands) was used for live/dead staining according to the manufacturer's instructions. Antibodies used for analysis are described in supplementary table 1. Specific combinations used for cytometry panels are described in supplementary table 2.

SUPPLEMENTARY TABLE 1. Antibodies used

Antigen	Clone	Fluorophore	Vendor	Catalog no. (on 12-12-2017)
Lineage (CD3, CD14, CD16, CD19, CD20, CD56)	MφP9, NCAM16.2, 3G8, SK7, L27, SJ25C1	FITC	BD Biosciences	340546
CD1c	L161	PE-Cy7	ThermoFisher Scientific (eBioscience)	25-0015-41
CD3	OKT3	PerCP-Cy5.5	ThermoFisher Scientific (eBioscience)	45-0037-42
CD3	OKT3	PE	BD Biosciences	16-0037-81
CD3	UCHT1	BV421	BD Biosciences	562427/562427
CD4	OKT4	PerCP-Cy5.5	ThermoFisher Scientific (eBioscience)	45-0048-42
CD8a	RPA-T8	APC-eFlour 780	ThermoFisher Scientific (eBioscience)	47-0088-42
CD11b	ICRF44	PE	ThermoFisher Scientific (eBioscience)	12-0118-41
CD11c	BU15	APC-eFlour 780	ThermoFisher Scientific (eBioscience)	47-0128-41
CD14	61D3	APC	ThermoFisher Scientific (eBioscience)	17-0149-42
CD18	6.7	FITC	ThermoFisher Scientific (eBioscience)	11-0189-42
CD27	9F4	FITC	Sanquin	M1764
CD28	CD28.2	PerCP-Cy5.5	ThermoFisher Scientific (eBioscience)	45-0289-41
CD30	BerH8	PE	BD Biosciences	550041
CD33	WM53	PE-Cy7	ThermoFisher Scientific (eBioscience)	25-0338-42
CD38	HB7	PE-Cy7	ThermoFisher Scientific (eBioscience)	25-0388-41
CD45RA	HI100	APC	ThermoFisher Scientific (eBioscience)	17-0458-42/41
CD54	HA58	APC	ThermoFisher Scientific (eBioscience)	17-0549-41
CD69	FN50	FITC	ThermoFisher Scientific (eBioscience)	11-0699-41
CD95	DX2	PE-Cy7	BD Biosciences	561636
CD103	BerACT8	FITC	BD Biosciences	561677
CD123	7G3	PerCP-Cy5.5	BD Biosciences	560904
CD134 (OX40)	ACT35	PE-Cy7	BD Biosciences	563663
CD137	4B4	PE	ThermoFisher Scientific (eBioscience)	12-1379-42
CD141	1A4	PE	BD Biosciences	559781
CD183 (CXCR3)	CEW33D	PE-Cy7	ThermoFisher Scientific (eBioscience)	25-1839-42
CD195 (CCR5)	NP-6G4	APC	ThermoFisher Scientific (eBioscience)	17-1956-41
CD197 (CCR7)	150503	BV421	BD Biosciences	562555
CD270 (HVEM)	94801	Alexa Fluor 647	BD Biosciences	564411
CD272 (BTLA)	J168-540	APC	BD Biosciences	564800
CD278 (ICOS)	DX29	BV421	BD Biosciences	562901
CD274 (PD1)	MIH4	PE	ThermoFisher Scientific (eBioscience)	12-9969-41
CD357 (GITR)	eBioAITR	PE-Cy7	ThermoFisher Scientific (eBioscience)	25-5875-41
HLA-DR	G46-6	BV421	BD Biosciences	562804
T-bet	eBio4B10	eFluor 660	ThermoFisher Scientific (eBioscience)	55-5825-80
Eomesodermin	WD1928	PE-Cy7	ThermoFisher Scientific (eBioscience)	25-4877-41
FOXP3	236A/E7	FITC	ThermoFisher Scientific (eBioscience)	11-4777-41

When indicated, PBMCs were pre-activated prior to phenotyping using anti-CD3/anti-CD28 beads (Life Technologies) and 100 U/mL IL-2. Flow cytometry was performed on a BD FACSVerse (BD Biosciences) and samples were analysed with Premium Cytobank software (cytobank.org). Each cytometry panel indicated in supplementary table 2 was analysed separately by CITRUS comparing baseline PBMCs to PBMCs after 3 and 6 cycles of chemotherapy (3 time points total). For analysis by CITRUS, the following parameters were used: 95000 total events were clustered at 5000 sampled events per file. Minimum cluster size was set at 2.3% with an FDR of 1%. Where indicated, additional t-SNE analysis was performed to visualize the data. For analysis by t-SNE, the viSNE function was used with the following parameters: ~60.000 total events were sampled using proportional sampling from across all files. ViSNE was run using 1000 iterations, a perplexity of 30 and theta of 0.5.

SUPPLEMENTARY TABLE 2. Antibody panels used

Panel 1	Panel 2	Panel 3	Panel 4	Panel 5	Panel 6	Panel 7	Panel 8
CD3	HLA-DR	HLA-DR	CD3	CD3	CD3	CD3	CD3
CD8a	CD11b	Lineage	CD8a	CD8a	CD8a	CD8a	CD8a
CD4	CD33	CD141	CD4	CD4	CD27	CD4	CD4
CD45RA	CD14	CD123	CD69	CD18	CD30	CD30	FOXP3
CD27	CD11c	CD1c	CCR5	CD54	GITR	OX40	Eomesodermin
CCR7		CD11c	CD137	PD1	ICOS	HVEM	Tbet
CD95			CD38	CXCR3	BTLA	CD103	Ki-67

Statistics

All statistical analyses were performed using built-in cytobank analysis (CITRUS), or Graphpad Prism for data obtained by manual gating. For data that was gated manually, all tests were performed by two-sided non-parametric t-tests or Friedman with Dunn's post-test, and p-values <0.05 were considered significant.

ACKNOWLEDGEMENTS

This work was supported by Dutch Cancer Society/Alped'Huzes grant UMCG 2014–6719 to MB, Jan Kornelis de Cock Stichting grants to FLK, KLB and FAE, Dutch Cancer Society grant RuG2012-5557 to NL and a UMCG Mandema Stipend to NL.

The authors would like to thank Henk Moes and Geert Mesander for their technical assistance.

REFERENCES

1. Vaughan S, Coward JI, Bast RC, Berchuck A, Berek JS, Brenton JD, Coukos G, Crum CC, Drapkin R, Etemadmoghadam D, Friedlander M, Gabra H, Kaye SB, Lord CJ, et al. Rethinking ovarian cancer: recommendations for improving outcomes. Nat Publ Gr [Internet]. 2011 [cited 2017 Aug 8];11.

2. Leffers N, Gooden MJM, de Jong RA, Hoogeboom B-N, ten Hoor KA, Hollema H, Boezen HM, van der Zee AGJ, Daemen T, Nijman HW. Prognostic significance of tumor-infiltrating T-lymphocytes in primary and metastatic lesions of advanced stage ovarian cancer. Cancer Immunol Immunother [Internet]. 2009 [cited 2016 Mar 22];58:449–59.

3. Vermeij R, de Bock GH, Leffers N, Ten Hoor KA, Schulze U, Hollema H, van der Burg SH, van der Zee AGJ, Daemen T, Nijman HW. Tumor-infiltrating cytotoxic T lymphocytes as independent prognostic factor in epithelial ovarian cancer with wilms tumor protein 1 overexpression. J Immunother [Internet]. [cited 2016 Mar 22];34:516–23.

4. Hwang W-T, Adams SF, Tahirovic E, Hagemann IS, Coukos G. Prognostic significance of tumor-infiltrating T cells in ovarian cancer: a meta-analysis. Gynecol Oncol [Internet]. 2012 [cited 2016 Mar 22];124:192–8. Available from: http://www.ncbi.nlm.nih.gov/pubmed/22040834

5. Barnes TA, Amir E. HYPE or HOPE: the prognostic value of infiltrating immune cells in cancer. Br J Cancer [Internet]. 2017 [cited 2017 Aug 8];

6. Nelson BH. The impact of T-cell immunity on ovarian cancer outcomes. Immunol Rev [Internet]. 2008;222:101–16.

7. Sato E, Olson SH, Ahn J, Bundy B, Nishikawa H, Qian F, Jungbluth AA, Frosina D, Gnjatic S, Ambrosone C, Kepner J, Odunsi T, Ritter G, Lele S, et al. Intraepithelial CD8+ tumor-infiltrating lymphocytes and a high CD8+/regulatory T cell ratio are associated with favorable prognosis in ovarian cancer. Proc Natl Acad Sci U S A [Internet]. 2005 [cited 2015 Jan 18];102:18538–43.

8. Wouters MCA, Komdeur FL, Workel HH, Klip HG, Plat A, Kooi NM, Wisman GBA, Mourits MJE, Arts HJG, Oonk MHM, Yigit R, de Jong S, Melief CJM, Hollema H, et al. Treatment Regimen, Surgical Outcome, and T-cell Differentiation Influence Prognostic Benefit of Tumor-Infiltrating Lymphocytes in High-Grade Serous Ovarian Cancer. Clin Cancer Res [Internet]. 2016 [cited 2016 Dec 1];22:714–24.

9. Wouters MCA, Komdeur FL, de Bruyn M, Nijman HW. Size matters: Survival benefit conferred by intratumoral T cells is dependent on surgical outcome, treatment sequence and T cell differentiation. Oncoimmunology [Internet]. 2016 [cited 2016 Dec 1];5:e1122863.

10. Tumeh PC, Harview CL, Yearley JH, Shintaku IP, Taylor EJM, Robert L, Chmielowski B, Spasic M, Henry G, Ciobanu V, West AN, Carmona M, Kivork C, Seja E, et al. PD-1 blockade induces responses by inhibiting adaptive immune resistance. Nature [Internet]. 2014 [cited 2014 Nov 26];515:568–71.

11. Karyampudi L, Lamichhane P, Krempski J, Kalli KR, Behrens MD, Vargas DM, Hartmann LC, Janco JMT, Dong H, Hedin KE, Dietz a. B, Goode EL, Knutson KL. PD-1 blunts the function of ovarian tumor-infiltrating dendritic cells by inactivating NF-KappaB. Cancer Res [Internet]. 2015.

12. Landskron J, Helland Ø, Torgersen KM, Aandahl EM, Gjertsen BT, Bjørge L, Taskén K. Activated regulatory and memory T-cells accumulate in malignant ascites from ovarian carcinoma patients. Cancer Immunol Immunother [Internet]. 2015;64:337–47.

13. Teng MWL, Ngiow SF, Ribas a., Smyth MJ. Classifying Cancers Based on T-cell Infiltration and PD-L1. Cancer Res [Internet]. 2015;75:2139–45.

14. Khagi Y, Kurzrock R, Patel SP. Next generation predictive biomarkers for immune checkpoint inhibition. Cancer Metastasis Rev [Internet]. Springer US; 2017 [cited 2017 Aug 17];36:179–90.

15. Wang D, Guo L, Wu X. Checkpoint inhibitors in immunotherapy of ovarian cancer. Tumor Biol [Internet]. 2014;36:33–9.

16. Wouters MCA, Komdeur FL, Workel HH, Klip HG, Plat A, Kooi NM, Wisman GBA, Mourits MJE, Arts HJG, Oonk MHM, Yigit R, de Jong S, Melief CJM, Hollema H, et al. Treatment Regimen, Surgical Outcome, and T-cell Differentiation Influence Prognostic Benefit of Tumor-Infiltrating

Lymphocytes in High-Grade Serous Ovarian Cancer. Clin Cancer Res [Internet]. 2016 [cited 2016 Mar 22];22:714–24.

17. Komdeur FL, Wouters MCA, Workel HH, Tijans AM, Terwindt ALJ, Brunekreeft KL, Plat A, Klip HG, Eggink FA, Leffers N, Helfrich W, Samplonius DF, Bremer E, Wisman GBA, et al. CD103+ intraepithelial T cells in high-grade serous ovarian cancer are phenotypically diverse TCRαβ+ CD8αβ+ T cells that can be targeted for cancer immunotherapy. Oncotarget [Internet]. 2016 [cited 2016 Dec 1].

18. Lo CS, Sanii S, Kroeger DR, Milne K, Talhouk A, Chiu DS, Rahimi K, Shaw PA, Clarke BA, Nelson BH. Neoadjuvant Chemotherapy of Ovarian Cancer Results in Three Patterns of Tumor-Infiltrating Lymphocyte Response with Distinct Implications for Immunotherapy. Clin Cancer Res [Internet]. 2017 [cited 2018 Jan 21];23:925–34.

19. Bruggner R V, Bodenmiller B, Dill DL, Tibshirani RJ, Nolan GP. Automated identification of stratifying signatures in cellular subpopulations. Proc Natl Acad Sci U S A [Internet]. National Academy of Sciences; 2014 [cited 2017 Mar 21];111:E2770-7.

20. Welters MJ, Van Der Sluis TC, Van Meir H, Loof NM, Van Ham VJ, Van Duikeren S, Santegoets SJ, Arens R, De Kam ML, Cohen AF, Van Poelgeest MI, Kenter GG, Kroep JR, Burggraaf J, et al. Vaccination during myeloid cell depletion by cancer chemotherapy fosters robust T cell responses.

21. Komdeur FL, Prins TM, van de Wall S, Plat A, Wisman GBA, Hollema H, Daemen T, Church DN, de Bruyn M, Nijman HW. CD103+ tumor-infiltrating lymphocytes are tumor-reactive intraepithelial CD8+ T cells associated with prognostic benefit and therapy response in cervical cancer. Oncoimmunology. 2017;

22. Yoshihama T, Nomura H, Iwasa N, Kataoka F, Hashimoto S, Nanki Y, Hirano T, Makabe T, Sakai K, Yamagami W, Hirasawa A, Aoki D. Efficacy and safety of dose-dense paclitaxel plus carboplatin as neoadjuvant chemotherapy for advanced ovarian, fallopian tube or peritoneal cancer. Jpn J Clin Oncol [Internet]. 2017 [cited 2018 Jan 21];47:1019–23.

23. Summers C, Rankin SM, Condliffe AM, Singh N, Peters AM, Chilvers ER. Neutrophil kinetics in health and disease. Trends Immunol [Internet]. Elsevier; 2010 [cited 2018 Jan 22];31:318–24.

24. Yang J, Zhang L, Yu C, Yang X-F, Wang H. Monocyte and macrophage differentiation: circulation inflammatory monocyte as biomarker for inflammatory diseases. Biomark Res [Internet]. BioMed Central; 2014 [cited 2018 Jan 22];2:1.

25. Farber DL, Yudanin NA, Restifo NP. Human memory T cells: generation, compartmentalization and homeostasis. Nat Rev Immunol [Internet]. NIH Public Access; 2014 [cited 2018 Jan 22];14:24–35.

26. Wu L, Deng Z, Peng Y, Han L, Liu J, Wang L, Li B, Zhao J, Jiao S, Wei H, Wu L, Deng Z, Peng Y, Han L, et al. Ascites-derived IL-6 and IL-10 synergistically expand CD14+HLA-DR low myeloid-derived suppressor cells in ovarian cancer patients. Oncotarget [Internet]. Impact Journals; 2017 [cited 2018 Jan 21];8:76843–56.

27. Dijkgraaf EM, Heusinkveld M, Tummers B, Vogelpoel LTC, Goedemans R, Jha V, Nortier JWR, Welters MJP, Kroep JR, van der Burg SH. Chemotherapy alters monocyte differentiation to favor generation of cancer-supporting M2 macrophages in the tumor microenvironment. Cancer Res [Internet]. 2013 [cited 2018 Jan 21];73:2480–92.

28. Polk A, Svane I-M, Andersson M, Nielsen D. Checkpoint inhibitors in breast cancer – Current status. Cancer Treat Rev [Internet]. 2018 [cited 2018 Jan 21];63:122–34.